Computational Materials Science 201 (2022) 110909

Contents lists available at ScienceDirect

Computational Materials Science

journal homepage: www.elsevier.com/locate/commatsci

Molecular modeling of methacrylic composite materials doped with nonlinear optical azochromophores with various acceptor fragments

O.D. Fominykh *, A.V. Sharipova, M.Yu. Balakina

Arbuzov Institute of Organic and Physical Chemistry, FRC Kazan Scientific Center, Russian Academy of Sciences, Arbuzov str. 8, 420088 Kazan, Russian Federation

ARTICLE INFO

Keywords:
Azochromophores
Noncovalent interactions
Hydrogen bonding
Molecular modeling
(co)methacrylic polymers

ABSTRACT

The methacrylate-based composite polymer materials with various weight content of azochromophores-guests – aminoazobenzenes with various acceptor moieties: AAB-NO_2, AAB-DCV, AAB-TCV, and AAB-TCP, – are studied by atomistic modeling. Polymer matrices are PMMA, copolymer of methyl methacrylate and methacrylic acid, MMA-MAA, and copolymer MMA-MAZ, MAZ unit containing azochromophore, covalently attached to the side chain via spacer. The realization of various non-covalent interactions (hydrogen and π-π interactions) is considered, special emphasis is given to the role of chromophore structure and polymer matrix nature.

It is shown that rather uniform distribution of chromophores in composite materials is retained even at 30 wt% content. In all composites with chromophore content growth both the number of non-covalently bound chromophores and the proportion of chromophores bound inter se increase, while the proportion of chromophores, bound with polymer matrix, decreases.

The number of hydrogen bonds (HBs) between chromophores-guests is determined mostly by the nature of the acceptor group of the chromophore, maximum number of HBs being formed by AAB-TCP. The MMA-MAA matrix allows realization of greater number of inter-chain HBs compared to MMA-MAZ matrix, while such bonds are absent in PMMA.

Azochromophores in MAZ units of MMA-MAZ matrix form π-π-stacking structures with mostly codirected chromophore dipole moments, besides AAB-TCV guests form such stacking structures with host matrix chromophores. Chromophores in MAZ units more easily interact with guests than with each other via π-π stacking. The studied matrices could be considered promising to be used as hosts at developing composite materials with quadratic nonlinear optical response.

1. Introduction

At present there exists an urgent need for constructing photonic devices for transmission and storage of large amounts of information, such as high speed signal modulators, converters, and switches, which require the development of new materials with ultra-low energy consumption and ultra-high speed wide bandwidth, low control voltage, low optical losses; such materials must be inexpensive and well compatible with other materials used in device design [1–6]. Organic polymer materials satisfy these requirements; they are able to provide a high and stable in time nonlinear-optical (NLO) response, which is formed at the molecular level due to organic NLO chromophores introduced into the polymer matrix either as guest molecules or as fragments covalently attached to the bearing chain [7]. Various strategies were developed to improve chromophores poling efficiency in achieving non-centrosymmetric chromophore organization necessary to exhibit quadratic NLO response [1-3,7] along with thermal stability in poled films of guest–host polymers; in particular, the introduction of isolation groups into different components of the chromophores [8], the use of bichromophore NLO units [9], the self-assembly strategy of supramolecular organization of chromophores with dendritic moieties through dipole–dipole stacking [10,11], binary chromophores application [12] etc. During recent decades great efforts of the researchers were focused on the development of new effective organic chromophores; however, one of the key problems in this field of research remains the search for the way of optimal transfer of molecular nonlinearity to the macroscopic one [13]. The solution of this problem is complicated by the fact that the experimental data on the quadratic NLO susceptibilities are measured in condensed matter where the molecular properties are affected by the host matrix, and it is impossible to separate the physical

* Corresponding author.
E-mail addresses: fod5@yandex.ru (O.D. Fominykh), a.v.sharipova@yandex.ru (A.V. Sharipova), mbalakina@yandex.ru (M.Yu. Balakina).

https://doi.org/10.1016/j.commatsci.2021.110909
Received 26 May 2021; Received in revised form 8 September 2021; Accepted 21 September 2021
Available online 2 October 2021

properties of components. Molecular simulations can help to reveal various non-covalent interactions, analyze their role in providing long-term relaxation stability, explain their nature and separate different contributions to the macroscopic NLO response [14].

Molecular modeling has become a practical and important tool for polymer scientists making a step to consider condensed matter features and processes; in the early period – at the turn of the 20th and 21st centuries, it contributed to obtaining a number of important results: it was shown that for chromophores with high dipole moment and first hyperpolarizability, there exists optimal concentration providing maximal NLO response [15,16]; the dynamics of the polarization process and the influence of the orienting field on the relaxation of the NLO response in composite polymer systems based on polymethyl methacrylate (PMMA) host and various chromophores was studied [17–19]; the simulation of the effect of the applied electric field on chromophores orientation in PMMA and amorphous polycarbonate matrices was performed by Monte-Carlo technique with the account of electrostatic chromophore interactions [20,21], as well as by the molecular dynamics in epoxy polymers with chromophores in the main [22] or side chain [23]. Our previous research [24] considered molecular mobility in copolymer of methyl methacrylate MMA and MAZ, MMA-MAZ, MAZ unit containing covalently attached azochromophore with nitro-group as acceptor [25], and estimation of glass transition temperature, T_g, for the systems of different size, the effect of chromophore concentration and the presence of the isolation groups on the homogeneity of chromophores distribution and aggregation in PMMA-based guest–host material [26,27]. Modern research devoted to the modeling of NLO phenomena in guest–host systems are reviewed in [28,29].

In design of polymer materials with quadratic NLO activity very important role belongs to non-covalent interactions. These interactions affect the efficiency of establishing the noncentrosymmetric organization of chromophores during poling [7]. Non-covalent interactions can contribute to long-term stability of the material's NLO response due to the preservation of the orientation order of chromophores established at the poling stage; both polymer chains and the chromophores-guests themselves can participate in such bonding. NLO polymers mostly comprise the guest–host structures, where the host polymers hold the guest chromophores in a fixed position by non-covalent interactions [30].

Theoretical study of non-covalent interactions of various kinds – hydrogen bonding, π-π stacking, van-der-Waals interactions – is generally performed for molecular systems of the limited size, in particular, dimers [31–34]. This falls considerably short of the scales at which we would like to understand structural peculiarities and chromophore concentration dependencies in NLO materials where non-covalent interactions play an appreciable role [35]. The impact of the strength of the non-covalent interaction on the optical response of the material characterized by supramolecular complexation between photo-responsive azobenzene chromophores and a photopassive polymer host is considered in [36]. The way for analysis and visualization of non-covalent interactions is developed in [37,38] based on computational algorithms and their implementation.

Polymer matrices to be used in the production of the NLO materials should meet the requirements of high thermal stability and optical transparency [3,39]. PMMA matrices are frequently applied as hosts for composite polymer NLO materials [7], although they have a relatively low T_g, high optical transparency and low optical losses. Other methacrylate-based matrices, such as copolymers of MMA and methacrylic acid (MAA), MMA-MAA, can also serve as host matrix; in [40] the study of linear-dendritic poly(methyl methacrylate)-dendron block copolymer with chromophores coupled via HBs was described.

Here we study the possibility of the formation of physical network via Hydrogen-bonding between different components of composite polymer materials by molecular modeling. The effect of the chromophores-guests concentration and structure, in particular, the nature of acceptor moieties: nitro-, AAB-NO_2 (Fig. 1a), dicyanovinylene, AAB-DCV (Fig. 1b), tricyanovinylene, AAB-TCV (Fig. 1c), and tricyanopyrrole, AAB-TCP (Fig. 1d) as well as the nature of host methacrylic matrices– PMMA (Fig. 1e), copolymer MMA-MAA (Fig. 1f), and MMA-MAZ (Fig. 1g) – on the realization of various types of non-covalent bonds is analyzed. It is worth stressing that MMA-MAZ is itself a chromophore-containg matrix, thus the effect of various ways of chromophores introduction into the material on the realization of different types of non-covalent interactions is revealed.

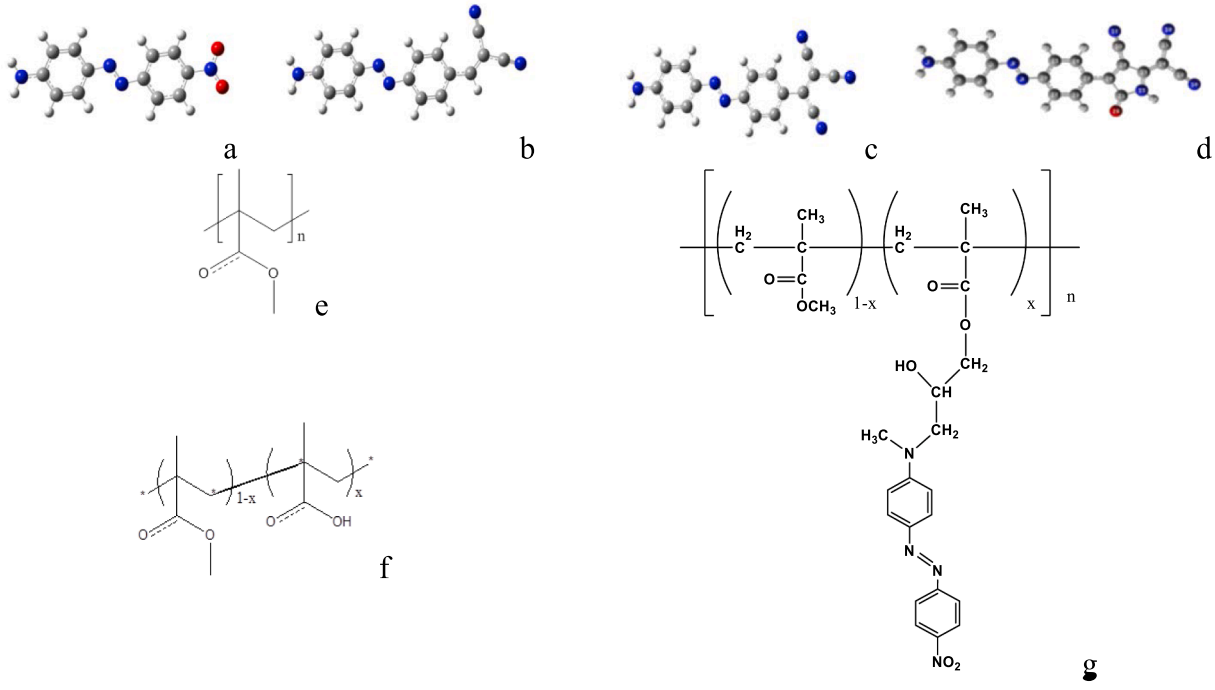

Fig. 1. Chromophores-guests AAB-NO_2 (a), AAB-DCV (b), AAB-TCV (c), AAB-TCP (d), monomer unit of PMMA (e), copolymers MMA-MAA (f), MMA-MAZ (g).

2. Materials and methods

All polymer matrices contain 10 chains of atactic (co)polymer with 60 units, for copolymer MMA-MAA the monomer units ratio is 9:1 (x = 0.1, Fig. 1) and for MMA-MAZ it is 4:1 (x = 0.2, Fig. 1). The monomer units are arranged so that MAA (MAZ) ones are never the neighbors. Chromophores-guests were added in 10, 20 and 30 wt% concentrations. The following composite systems were considered: PMMA/AAB-NO_2(10), PMMA/AAB-NO_2(20), PMMA/AAB-NO_2(30), PMMA/AAB-DCV(10), PMMA/AAB-DCV(20), PMMA/AAB-DCV(30), PMMA/AAB-TCV(20), MMA-MAA/AAB-NO_2(20), MMA-MAA/AAB-NO_2(30), MMA-MAA/AAB-TCP(20), MMA-MAA/AAB-TCP(30), and composite material with binary chromophores, MMA-MAZ/AAB-TCV(20), were number in round brackets means the chromophore weight content in composite material. Chromophores and polymer chains molecular weights are given in Table 1.

The molecular modeling was performed with OPLS3e force field, which is parameterized on the basis of high-level quantum chemical calculations [41,42]. Composite materials were packed in amorphous cell (compressive NPT protocol) in the course of multistage modeling, one of the stages is simulated annealing [43], when the system was heated up to 700 K and then cooled to 300 K. After relaxing the system, molecular dynamics at 400 K was performed for 20 ns with 1 fs timestep for all the systems. The temperature 400 K was chosen, since it is close to T_g for materials based on methacrylic polymer matrices; e.g., T_g for PMMA comprises 388 K [44], MMA-MAZ comprises 395 K [25]. Our previous research on the local mobility in MMA-MAZ copolymer demonstrated that at 400 K all molecular motions associated with γ-, β- and α- relaxation processes start [24]. We have assumed that simulation at this temperature is quite reasonable; moreover, it allows us to make the comparison of various composite systems uniform.

The details of multistage simulation workflow protocol are presented in Supplementary data, Table S1. The system is assumed relaxed when the variation of cohesive energy with time, the measure of stability, becomes insignificant (Fig. S1). The chromophores distribution in composite polymer material and various intermolecular bonds, both Hydrogen bonds (HB) and π-π stacking ones (between chromophores, between polymer chains and between chains and chromophores) were analyzed in the course of molecular dynamics (MD) and at the final stage. Variation of HB number in the course of molecular dynamics stage was analyzed separately for all considered here systems. The proportion of chromophores, bound with each other, is denoted as p^{cc}(HB) for H-bonded chromophores and $p^{cc}(\pi)$ for π-π linked chromophores; it is estimated as N_b/N – the ratio of the number of chromophores bound with each other, N_b, to the total number of chromophores in a cell, N; N_b(HB) – the number of H-bonded inter se chromophores, $N_b(\pi)$ the number of π-π linked chromophores. The proportion of chromophores bound to polymer chains is denoted correspondingly as p^{cm}(HB) and $p^{cm}(\pi)$. When we consider variation of HB number during 20 ns, we analyze the doubled value of p^{cc}(HB) for inter-chromophore bonding, thus we assume that chromophores are bound predominantly in pairs, what is shown to be true up to 20 wt% chromophore content.

The estimations of T_g were performed for MMA-MAZ/AAB-TCP and MMA-MAZ/AAB-TCV composites on the basis of a set of molecular dynamics simulations in the temperature range from 600 to 200 K with 10 K step in the NPT ensemble. Before the simulation the system was relaxed for 50 ns at 600 K; the polymer system equilibrated as a result of MD is used as a starting point. The specific volumes (1/density) are obtained from MD simulations at a set of temperatures in a wide temperature range starting from the polymer melting point. To obtain the thermophysical properties we used a bilinear fit: a linear regression is performed on the low temperature (glassy) region and the high temperature (rubbery) region of the plot of specific volume against temperature; T_g is the temperature at which the two regression lines or the two asymptotes meet.

The molecular modeling was performed with Materials Science Suite complex [45], which includes Desmond engine [46] for molecular dynamics calculations of material in amorphous cell.

Table 1
Molecular weights for the chromophore-guests.

Structure	Molecular weight, a.u.
chromophore	
AAB-NO_2	242.239
AAB-DCV	273.300
AAB-TCV	298.309
AAB-TCP	365.357
Polymer chain	
PMMA	6009.115
MMA-MAA	5840.789
MMA-MAZ	9290.437

3. Results and discussion

3.1. PMMA-based materials

3.1.1. PMMA/AAB-NO_2

Composite materials PMMA/AAB-NO_2(10), PMMA/AAB-NO_2(20), and PMMA/AAB-NO_2(30) were packed in amorphous cell; materials density, achieved in the course of packing, grew insignificantly with the increase of chromophore concentration and comprised 1.098, 1.118 and 1.140 g/cm^3, respectively. Chromophores are distributed in the material rather homogeneously even at 30 wt% content (see, for example, Fig. 2 (a,b)).

Chromophores are linked by HBs and π-π stacking interactions, the examples of chromophores clusters with centrosymmetric and non-centrosymmetric arrangement are given in Fig. 3 (a-c). Along with a large number of non-covalent HBs between chromophore amino- and nitro-groups, the bonds between chromophores and polymer chains are realized in the material with participation of amino-group hydrogens and PMMA carbonyl group oxygens (Fig. 3 (d,e)).

Peculiarities of chromophores non-covalent bonding, both HB and π-π-stacking, are presented in Table 2. It is worth mentioning that among chromophore clusters those with *head-to-tail* arrangement due to HB formation were revealed, such structures are known to provide the growth of molecular quadratic NLO characteristics [31–34].

In PMMA/AAB-NO_2(10) only 4 chromophores are bound non-covalently, in PMMA/AAB-NO2(20) 18 out of 62 chromophores are linked to each other, p^{cc} is about 1/3, while in PMMA/AAB-NO_2(30) 38 out of 106 chromophores are bound both by HBs and π-π interactions, p^{cc} achieves ~ 2/3 (Table 2).

Considering separately the number of H-bonded and π-π-bonded chromophores, one can see that at 10 and 20 wt% content the sum of N_b(HB) and $N_b(\pi)$ differs insignificantly from N_b, giving evidence that at such concentrations the chromophores are linked either by HBs or by π-π interactions, but at 30 wt% content the sum becomes significantly greater than N_b, – i.e. many chromophores are coupled both by HBs and π-π interactions.

In the course of MD stage, variation of the number of chromophores, H-bonded with each other and with polymer chains, was considered separately. In PMMA/NO_2(10) there were 26 bonds on average between chromophores and the matrix (Table 3), in PMMA/AAB-NO_2(20) the number of such HBs increased to 55, and in PMMA/AAB-NO_2(30) it became 80. In the case of PMMA/AAB-NO_2(20) total number of HBs ranges from 44 to 83 (Table 3), chromophores are mostly bound to polymer chains rather than with each other (55 bonds against 8). The variation of the number of HBs in the PMMA/AAB-NO_2(30) material during MD stage is given in Fig. 2(c); the number of HBs ranges from 89 to 129 (Table 2); total average number of bonds (108) can be divided into bonds between the chromophores (28) and chromophores and polymer matrix (80).

The increase of chromophore content in a series PMMA/AAB-

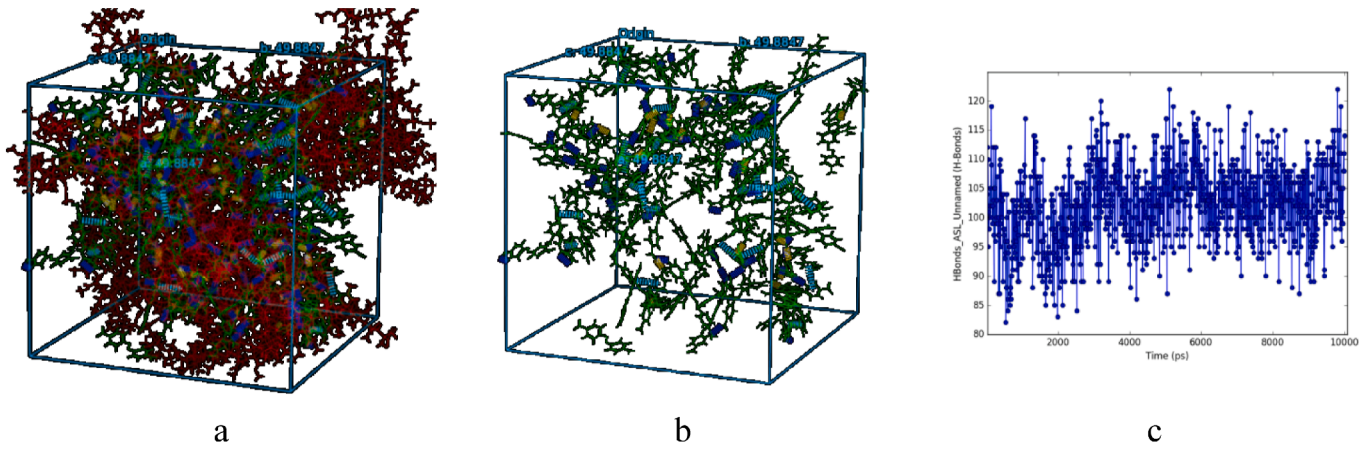

Fig. 2. Composite material PMMA/AAB-NO_2(30) packed in amorphous cell (a); chromophores distribution (for convenience polymer chains are hidden) (b); HB number variation with time (c).

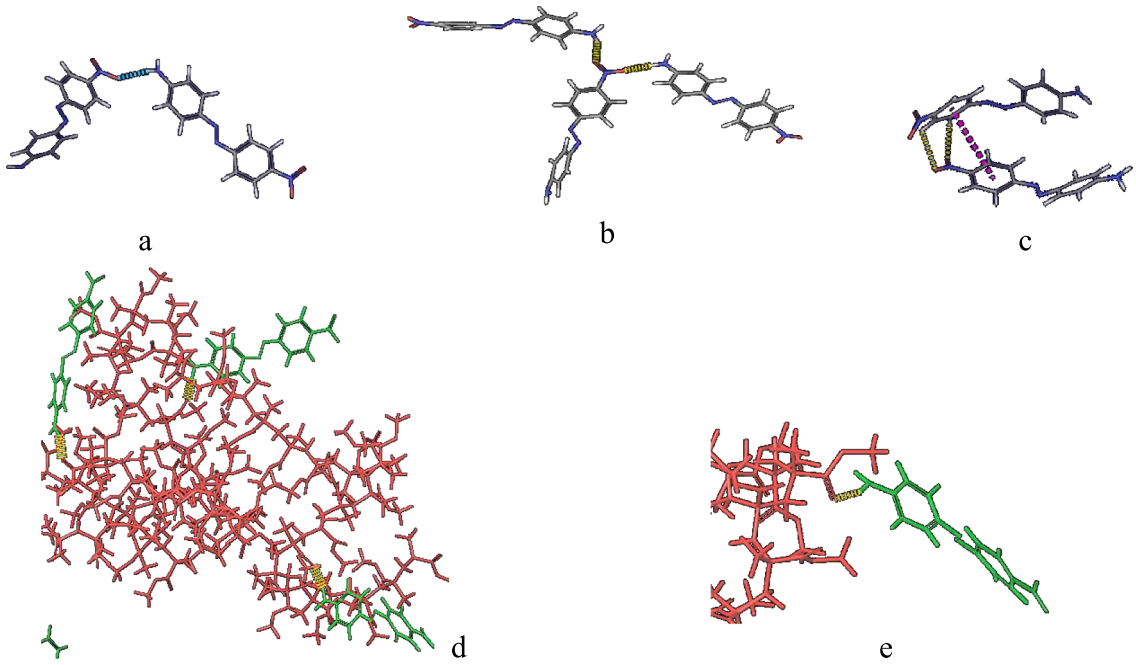

Fig. 3. Non-covalent bonds between chromophores: HB (a) and (b); π-π-stacking and aromatic HBs (c); HBs between chromophores and polymer chains (d,e) in PMMA/AAB-NO_2(30).

Table 2
A number and proportion of non-covalently bonded chromophores in PMMA-based composite materials.

	N	N_b	N_b(HB)	N_b(π)	p^{cc}, %	p^{cc}(HB), %	p^{cc}(π), %
PMMA/AAB-NO_2(10)	28	4	2	2	14	7	7
PMMA/AAB-NO_2(20)	62	18	4	18	29	6	29
PMMA/AAB-NO_2(30)	106	65	35	43	61	33	41
PMMA/AAB-DCV(10)	25	4	2	2	16	8	8
PMMA/AAB-DCV(20)	55	24	8	18	44	15	33
PMMA/AAB-DCV(30)	94	52	28	38	55	30	40
PMMA/AAB-TCV(20)	50	21	8	16	42	16	32

Table 3
Variation of HBs number in PMMA/AAB-NO_2(10), PMMA/AAB-NO_2(20) and PMMA/AAB-NO_2(30).

		PMMA/AAB-NO_2(10)	PMMA/AAB-NO_2(20)	PMMA/AAB-NO_2(30)
N		28	62	106
N_b(HB)	range	17–40	44–83	89–129
	mean	27	62	108
N_b^{cc}(HB)	range	0–5	1–15	16–40
	mean	1	8	28
	p^{cc}(HB), %	7	26	53
N_b^{cm}(HB)	range	17–38	41–74	64–99
	mean	26	55	80
	p^{cm}(HB), %	93	89	75

NO_2(10), PMMA/AAB-NO_2(20) and PMMA/AAB-NO_2(30) results in p^{cm}(H) decrease from 93 to 75%, while p^{cc}(H) grows from 7 to 53% (Table 3), demonstrating that even at 30 wt% content the chromophores are bound mostly with polymer chains rather than with each other. As for π-π-coupled chromophores, their proportion $p^{cc}(\pi)$ is always greater than p^{cc}(HB) at the same chromophore content and its growth is more pronounced than that of p^{cc}(HB); so chromophores are mostly bound inter se by π-π interactions, than by HBs (Table 2). It is worth stressing that no non-covalent bonds between PMMA chains were revealed.

3.1.2. Composites with cyano-containing chromophores as guests

In the case of composites PMMA/AAB-DCV the density of the material packed in the amorphous cell grows inessentially, achieving 1.084, 1.098 and 1.101 g/cm^3 with chromophore content increase from 10 to 30 wt%; this tendency is similar to that observed for PMMA/AAB-NO_2. In this case the homogeneous distribution of chromophores in the materials also preserves even at 30 wt% content (Fig. S2). Similar to the case of the materials with AAB-NO_2 guests, total number of HBs, N_b(HB), increases with the chromophore content growth (see Tables 2, 4).

In PMMA/AAB-DCV(10) 4 chromophores out of 25 are non-covalently bound with each other (Table 2), but only two of them form HB between nitrogen of azo-fragment and hydrogen of amino-group, another pair of chromophores are bound by π-π interactions. In PMMA/AAB-DCV(20) 24 out of 55 chromophores participate in non-covalent binding; some chromophores form associates of 3 or even 4 units due to HBs (Fig. 4 (a)); 18 chromophores are bound by π-π interactions, forming dimers and one trimer (Fig. 4(b)). Some chromophores are involved both in HB and π-π bonding. In PMMA/AAB-DCV (30) 52 out of 94 chromophores are bound inter se, many of them both by HBs and π-π interactions. Thus in PMMA/AAB-DCV(20) 44% of chromophores are bound inter se, while in the case of 30 wt% content p^{cc} achieves ~ 60% both for PMMA/AAB-NO_2(30) and PMMA/AAB-DCV(30). In PMMA/AAB-DCV(30) chromophore aggregates formed due to HBs and π-π interactions are revealed, the largest one includes 5 AAB-DCV chromophores (Fig. 4 (c)), what can be treated as the sign of the aggregation beginning. As for HBs between chromophores, their proportion p^{cc}(HB) becomes rather notable only at 30 wt% content (Tables 2-4). Similar to the case of PMMA/AAB-NO_2, p^{cc}(HB) increases from 8% to 62% with concentration, and p^{cm}(HB) decreases from 84 to 56% (Table 4) in composite materials PMMA/AAB-DCV, although total number of HBs between chromophores and matrix increases with chromophore content growth. The number of π-π linked chromophores and $p^{cc}(\pi)$ is greater than the number of H-bonded chromophores and p^{cc}(HB) at any considered concentration of AAB-DCV; both $p^{cc}(\pi)$ and p^{cc}(HB) grow with chromophore content similar to the case of PMMA/AAB-NO_2 composites.

Similar to PMMA/AAB-NO_2 a large number of *head-to-tail* dimers have been found for PMMA/AAB-DCV materials. Such dimers, formed by the studied azochromophores with a donor amino group and various acceptor groups, as mentioned above, can contribute to the chromophores preorganization and thus promote the growth of the material NLO response [34].

In PMMA/AAB-DCV composites chromophores also form non-covalent bonds with polymer matrix – between the hydrogens of the amino groups and the oxygens of the carbonyl groups in the PMMA (see, for example, Fig. S3 (a)). There are also aromatic hydrogen bonds between the chromophores and the matrix (Fig. S3 (b)).

Composite material with another cyano-containing chromophore guest was also considered – PMMA/AAB-TCV(20) (Fig. S4). The density of material achieved 1.100 g/cm^3, what is quite close to that for PMMA/AAB-DCV(20).

All types of non-covalent bonds were also revealed (Table 2). HBs are also realized between the chromophores and chromophores and the matrix (Table 4), similar to the case of two other composite materials considered above (Fig. S5); the total number of bonds between chromophores and the matrix is 21, among them 8 chromophores are bound by 5 HBs and 16 chromophores – by π-π interactions, some chromophores are linked both by HBs and π-π stacking (Fig. S5(a)). Variation of the HBs number with time is presented in Table 4. The number of chromophores in PMMA/AAB-DCV(20) and PMMA/AAB-TCV(20) is quite close (55 and 50, correspondingly), and the number of bonds between chromophores and between chromophores and matrix (Table 2), as well as p^{cc}(HB), $p^{cc}(\pi)$ and p^{cm}(HB) is also close for these two systems (Tables 2-4). These observations are illustrated in the diagram (Fig. S6 (a)). For PMMA/AAB-NO_2(20), PMMA/AAB-DCV(20) and PMMA/AAB-TCV(20) $p^{cc}(\pi)$ is almost equal, while the p^{cc}(HB) is quite close only for PMMA/AAB-DCV(20) and PMMA/AAB-TCV(20), being significantly higher than that for PMMA/AAB-NO_2(20).

Thus, by the example of PMMA/AAB-NO_2 and PMMA/AAB-DCV materials (Fig. S6 (b) and (c)), it was shown that increase in the concentration of chromophores results in the growth of p^{cc}(HB) and decrease of p^{cm}(HB). The chromophores are mostly bound with each other by π-π interactions than by HBs at chromophore content 20 wt% and higher.

3.2. Composite materials based on MMA-MAA matrix

To clarify how matrix nature affects the number of non-covalent bonds in the material, composites with MMA-MAA matrix with AAB-NO_2 and AAB-TCP as guests were considered. Due to the presence of carbonyl group in MMA and in MAA hydroxyl group, one may expect realization of HBs in the material. MMA-MAA-based composites were packed in amorphous cell, the density of the MMA-MAA/AAB-NO_2(20) and MMA-MAA/AAB-NO_2(30) after packing was 1.13 g/cm^3 and 1.14 g/cm^3, correspondingly; as for MMA-MAA/AAB-TCP(20) and MMA-MAA/AAB-TCP(30), the density is also quite close (1.09 and 1.11 g/cm^3, respectively). Chromophores in both materials are rather homogeneously distributed (see, for example, Fig. S7), the exception is the case of MMA-MAA/AAB-NO_2(30) where chromophores clusters, formed due to π-π interactions involving up to 6 units were revealed due to high numerical content of chromophores in the material.

For MMA-MAA/AAB-NO_2 the increase of chromophore content from 20 to 30 wt% results in the growth of the number of non-covalently bound chromophores (Table 5), the p^{cc} changes from 50 to 61%. Considering the number and proportion of HBs variation during 20 ns (Table 6), one can see that mean p^{cc}(HB) grows from 43 to 50% with chromophore content, p^{cm}(HB) decreases insignificantly (from 85 to 78%) with the chromophore content growth (Fig. S8). These values indicate that almost each chromophore is non-covalently bound to polymer matrix.

In MMA-MAA/AAB-TCP materials p^{cc} increases very insignificantly (from 55 to 59%) with chromophore content growth, p^{cc}(HB) changes from 42 to 46% and $p^{cc}(\pi$-$\pi)$ – from 22 to 26% (Table 5). The mean number $N_b{}^{cc}$(HB) and p^{cc}(HB) (Table 6) increase almost 1.5 times when

Table 4
Variation of HBs number in PMMA/AAB-DCV(10), PMMA/AAB-DCV(20), PMMA/AAB-DCV(30) and PMMA/AAB-TCV(20).

		PMMA/AAB-DCV (10)	PMMA/AAB-DCV (20)	PMMA/AAB-DCV (30)	PMMA/AAB-TCV (20)
N		25	55	94	50
N_b(HB)	range	13–31	40–67	61–102	34–65
	mean	22	53	82	51
$N_b{}^{cc}$(HB)	range	0–7	1–13	17–41	1–18
	mean	1	7	29	9
	p^{cc}(HB), %	8	25	62	36
$N_b{}^{cm}$(HB)	range	12–30	33–59	33–70	29–58
	mean	21	46	53	42
	p^{cm}(HB), %	84	83	56	84

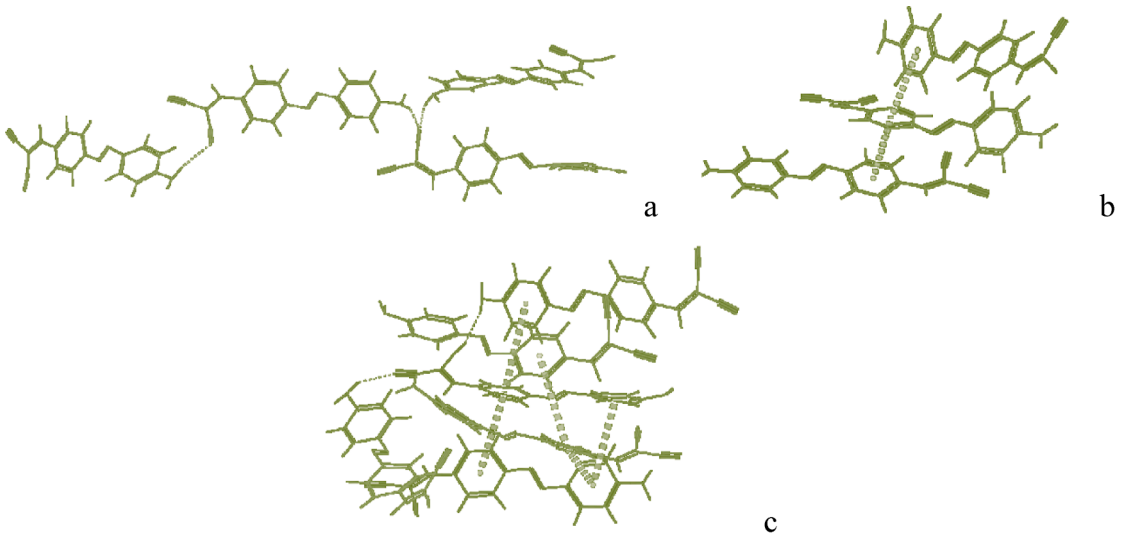

Fig. 4. Non-covalent interactions between chromophores: HBs (a), π-π interactions (b) in PMMA/AAB-DCV(20); π-π interactions in PMMA/AAB-DCV(30) (c).

Table 5
A number of non-covalently bonded inter se chromophores in MMA-MAA-based composite materials, p^{cc}, p^{cc}(HB), and $p^{cc}(\pi)$.

Composite system	N	N_b	N_b(HB)	$N_b(\pi)$	p^{cc}, %	p^{cc}(HB), %	$p^{cc}(\pi)$, %
MMA-MAA/ AAB-NO_2(20)	60	30	17	22	50	28	37
MMA-MAA/ AAB-NO_2(30)	103	63	31	50	61	30	29
MMA-MAA/ AAB-TCP(20)	40	22	17	9	55	43	23
MMA-MAA/ AAB-TCP(30)	69	41	32	18	59	46	26

Table 6
The number and proportion of HBs between definite components of composite materials MMA-MAA/AAB-NO_2 and MMA-MAA/AAB-TCP.

		MMA-MAA/ AAB-NO_2(20)	MMA-MAA/ AAB-NO_2 (30)	MMA-MAA/ AAB-TCP (20)	MMA-MAA/ AAB-TCP (30)
N		60	103	40	69
N_b(HB)	range	130–171	160–210	120–182	169–217
	mean	149	187	160	194
N_b^{mm}(HB)	range	70–98	62–103	61–84	57–80
	mean	84	80	73	69
N_b^{cc}(HB)	range	4–23	9–40	8–25	28–53
	mean	13	26	16	42
	p^{cc}(HB), %	43	50	80	122
N_b^{cm}(HB)	range	38–71	65–91	44–90	65–101
	mean	51	80	72	83
	p^{cm}(HB), %	85	78	180	120

chromophore content changes from 20 to 30 wt%, while the p^{cm}(HB) decreases 1.5 times, again giving evidence for the preference of inter-chromophore binding at high chromophore concentration in polymer composite material. In MMA-MAA/AAB-TCP(30) each chromophore is non-covalently bound both with another chromophore and with polymer chain.

Guest chromophores, as a rule, are connected by non-covalent interactions in pairs in MMA-MAA/AAB-TCP(20) (Fig. 5(a, b)), only in one case a tetramer is formed due to various interactions (Fig. 5 (c)). The number of HBs between polymer chains, N_b^{mm}(HB), decreases very insignificantly with chromophore content growth for all MMA-MAA-based composites considered here (Table 6), the number of HBs between chromophores, N_b^{cc}(HB), as well as between chromophores and the matrix, N_b^{cm}(HB), noticeably increases (Table 6, Fig. S9).

At the same wt.% content, p^{cc}(HB) is significantly greater for MMA-MAA/AAB-TCP than for MMA-MAA/AAB-NO_2, the same is true for p^{cm}(HB). The distinguishing feature of AAB-TCP chromophores is their ability to form HBs involving acceptor moieties – between polymer chain carbonyl group oxygens, cyano-group nitrogens and amino-group hydrogens (Fig. 6) – this acceptor has five sites for HB formation instead of two ones in AAB-NO_2. Such HBs between AAB-TCP acceptors could promote parallel arrangement of chromophores, what contributes to non-centrosymmetric chromophores preorganization.

The analysis of non-covalent bonding in these materials has shown that the total number of HBs in MMA-MAA/AAB-NO_2(20) and MMA-MAA/AAB-TCP(20) is quite close (149 and 160, respectively); in the MMA-MAA/AAB-NO_2(20), fewer bonds between chromophores and between chromophores and matrix were revealed, although the numerical content of chromophores is noticeably higher due to the difference in the chromophores weight (see Table 6, Table 1). The number of inter-chain HBs in MMA-MAA is close in all four considered systems, it does not depend on the chromophore concentration in composite material (Table 6).

It can be concluded that when AAB-NO_2 chromophores are guests, the number of non-covalent bonds in the material is noticeably less than in the case of AAB-TCP chromophores, despite the fact that the numerical content of AAB-NO_2 is 1.5 times higher than that of AAB- TCP with the same weight content in the material (Table S2). Chromophores AAB-TCP form significantly more bonds both with each other and with the matrix.

As can be seen from Table 6, p^{cm}(HB) decreases from 180% to 120% with chromophore content growth from 20 to 30 wt% for MMA-MAA/AAB-TCP, (see Fig. S8) – every chromophore is bound with polymer matrix at least with one bond; p^{cc}(HB) increases from 80 to 122% with chromophore content growth, i.e. the number of HB-ed chromophores increases linearly with chromophore content (1.5 times). As for MMA-MAA/AAB-TCP(30), each chromophore is bound to another one and with polymer chain.

Since PMMA and MMA-MAA chain lengths and weights are close (Table 1), and the numerical chromophore content in corresponding materials is quite close as well (Table S2), one may perform the comparison of PMMA-based and MMA-MAA-based composites with AAB-NO_2 chromophores-guests. The following observations can be made: i) the p^{cc} is greater in MMA-MAA/AAB-NO_2(20), than in PMMA/AAB-

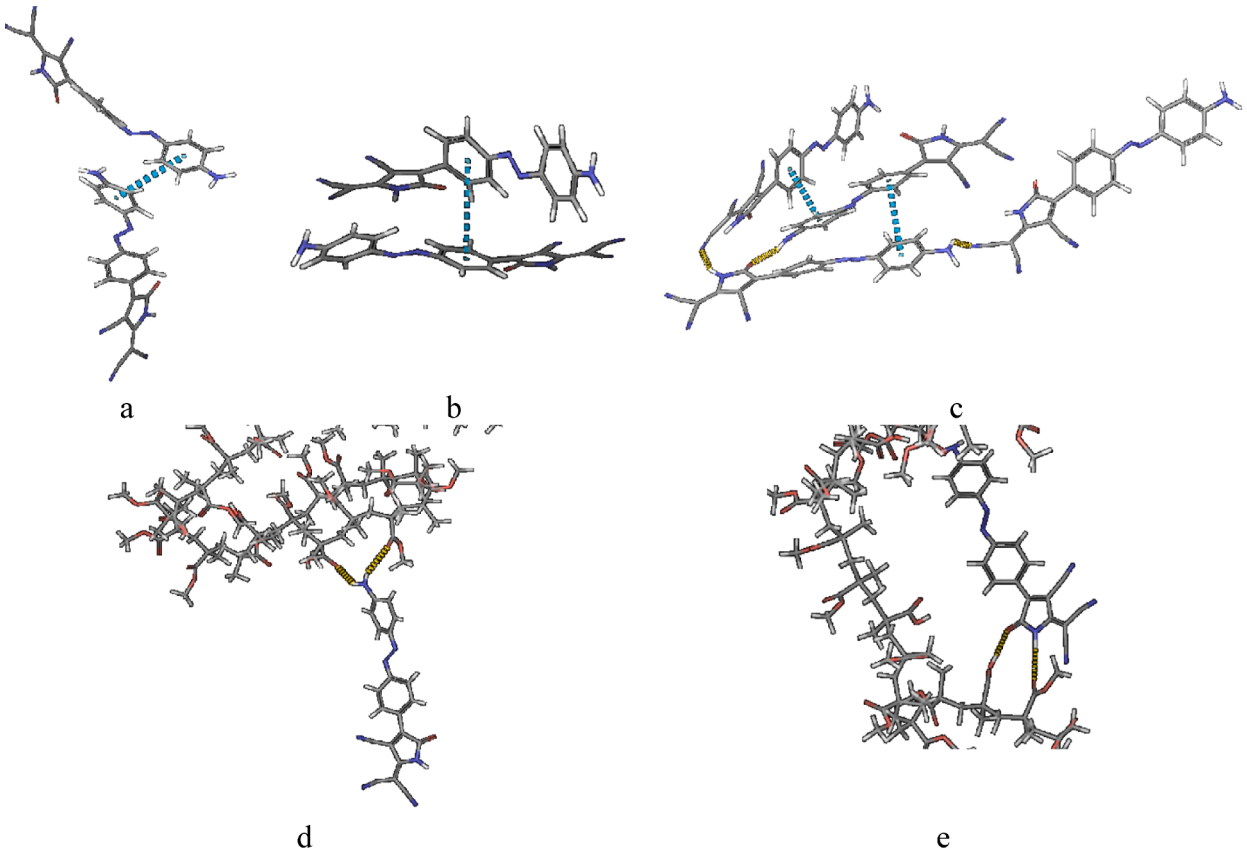

Fig. 5. Examples of coupling in MMA-MAA/AAB-TCP(20): π-π interactions between chromophore donor rings (a) and bridges (b); four chromophores coupled via π-π and HBs (c); HB between chromophores and polymer chains (d, e).

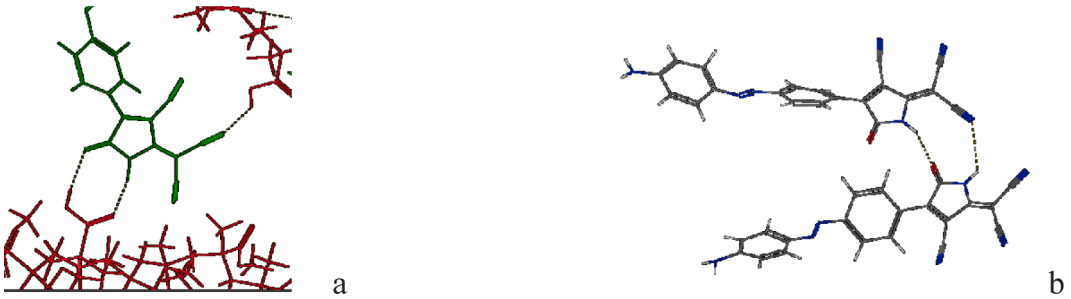

Fig. 6. HBs between AAB-TCP and MMA-MAA chain (MAA units) (a); HBs between AAB-TCP chromophores (b).

NO_2(20), the chromophores are bound by π-π interactions rather than by HBs in PMMA/AAB-NO_2(20), while in MMA-MAA/AAB-NO_2(20) the p^{cc}(π) is close to p^{cc}(HB), p^{cc} increases significantly for PMMA/AAB-NO_2(30) compared to PMMA/AAB-NO_2(20), but changes quite slightly for MMA-MAA/AAB-NO_2(30) (Tables 2 and 5); ii) p^{cc}(HB) is similar at the same chromophore content and increases with content growth for both types of composites, the same is true for the p^{cm}(HB) (Tables 3 and 6). Changes in the number of bonds during the simulation are visualized in the graphs given in Fig. S10.

3.3. Composite materials based on MMA-MAZ matrix

We have also considered composite materials with polymer matrix containing azochromophore covalently attached to the side chain via spacer group, MMA-MAZ (see Fig. 1 (g)); AAB-TCV chromophores (Fig. 1(c)) were introduced as guests with 20 wt% content (78 chromophores AAB-TCV and 120 chromophores in polymer matrix). After packing in the amorphous cell (Fig. S11 (a)) the material density was ~ 1.138 g/cm^3; chromophores AAB-TCV are rather uniformly distributed in the material (Fig. S11 (b)).

3.3.1. Guest-guest interactions

Chromophores-guests AAB-TCV are linked with each other through HBs and π-π bonds (Table 7), 27 chromophores out of 78 are linked by 19 HBs, and 23 chromophores out of 78 are linked by 17 π-π interactions, the largest aggregate contains 7 chromophores (Fig. 7); some chromophores are coupled both by HBs and π-π interactions; more than half of chromophores-guests are bound to each other, p^{cc} = 52% (Table 7).

3.3.2. Guest-host interactions

In MMA-MAZ/AAB-TCV(20) between the guest chromophores and the polymer matrix various HBs occur: these are the HBs between the oxygen of the nitro group of the azochromophore in MMA-MAZ and the hydrogen of the amino group in AAB-TCV, as well as the hydrogen of the amino group and oxygen of the carbonyl group of the matrix; an example of the latter is shown in Fig. S12. As for non-covalent π-π

Table 7
Number of chromophores, total number of bound chromopohres, HBs and π-π bonds between definite components of composite materials MMA-MAZ/AAB-TCV(20) and PMMA/AAB-TCV(20).

	MMA-MAZ/AAB-TCV(20)				PMMA/AAB-TCV(20)
	Chromophore-chromophore AAB-TCV–AAB-TCV	Chromophore-matrix AAB-TCV-MAZ		Matrix-matrix MAZ-MAZ	Chromophore-chromophore AAB-TCV-AAB-TCV
N(AAB-TCV)/N(MAZ)	78	78		120	50
N(total)			198		
N_b	41	36		26	21
N_b(HB)	27	29			8
N_b(π)	23	28	56	26	16
p^{cc},%	52	46			42
p^{cc}(HB)/p^{cm}(HB), %	34	37			16
p^{cc}(π)/p^{cm}(π)/p^{mm}(π) , %	29	36	28	22	32

coupling between AAB-TCV and MAZ units, 28 chromophores AAB-TCV are bound to MAZ (Table 7), some chromophores form stacking-pairs via two bonds (Table 7, Fig. S13). Only one AAB-TCV chromophore was revealed, that was involved both in π-π bonding with another AAB-TCV and MAZ unit simultaneously. As it can be seen from Table 7, the number (and proportion) of chromophore-guests AAB-TCV bound to MAZ units via π-π interactions, is somewhat greater, than the number of chromophores-guests, bound to each other (28 against 23, $p^{cm} = 36$, $p^{cc} = 29$) due to the greater number of MAZ units against the number of AAB-TCV chromophores-guests.

3.3.3. *Host-host interactions*

Between fragments of the polymer matrix both HBs and π-π bonds are again revealed. HBs are most frequently realized between hydroxyl and carbonyl groups belonging to the same chain or even to the same MAZ unit (Fig. 8(a)), as well as between OH groups of MAZ and C = O groups of MMA (Fig. 8(b)), between OH groups of MAZ fragments (Fig. S13(a)); nitro-groups in chromophore fragments in MAZ units can form HBs with OH group in spacer, but only a single HB of such type was revealed (Fig. S14(b)). Chromophores in MAZ units are coupled by π-π bonds (Fig. 8 (c)); 26 out of 120 chromophores in MAZ units are bound inter se (Table 7). Chromophores in MAZ units form stacking structures via donor–donor or donor–acceptor interactions predominantly with co-directed chromophore dipole moments.

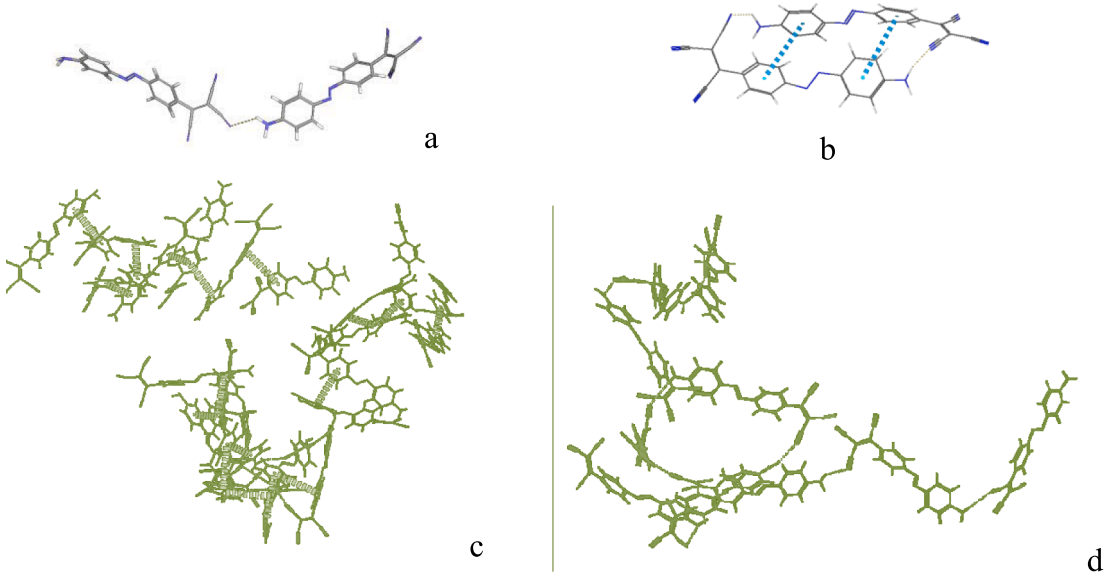

Fig. 7. Non-covalent bonds between AAB-TCV: HBs (a), π-π-stacking (b), clusters formed by π-π interactions (c) and HBs (d).

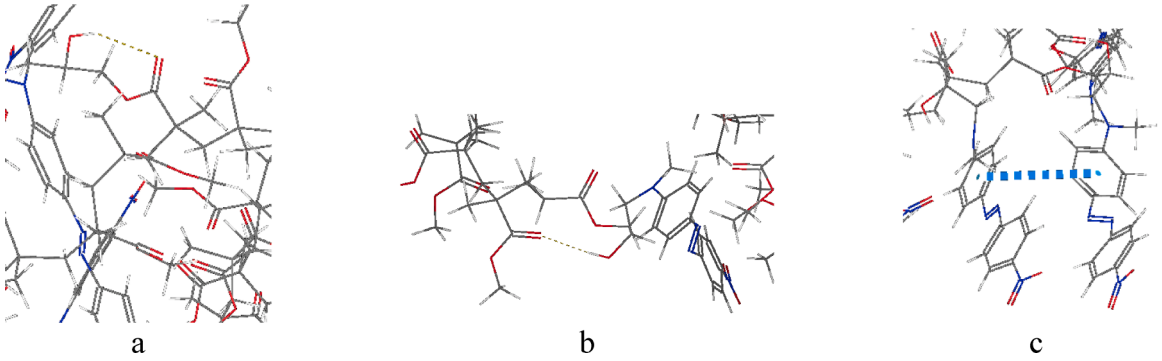

Fig. 8. Examples of non-covalent bonds between polymer chains: HBs between hydroxyl groups and carbonyl group in MAZ spacer (a); HBs between MMA carbonyl group and MAZ hydroxyl group(b); π-π interactions between MAZ chromophores (c).

Summarizing these observations one can conclude, that chromophores-guests more easily interact with each other ($p^{cc} = 52\%$), than with chromophores in MAZ units in polymer chains ($p^{cm} = 46\%$). The statistical analysis of HBs in MMA-MAZ/AAB-TCV is given in Table 8 and Fig. S15, where the variation range and mean values of bond numbers are presented.

Largest number of HBs is formed between AAB-TCV guests and MAZ units (49 bonds, corresponding to ~ 63% of guests), the chromophores-guests form only 22 bonds (44 chromophores AAB-TCV interact with each other via HBs), and 35 HBs are formed between polymer chains. Assuming the pairwise binding, the number of AAB-TCV chromophores bound inter se and with polymer chains are similar. The radial distribution functions (RDF) for H-bonded atoms are obtained (Fig. S16) confirming the preservation of hydrogen bonds in composite material at elevated temperature. The non-covalent bonds in MMA-MAZ may serve a so-called physical network, which could contribute to relaxation stability of chromophores ordering.

3.3.4. *Comparison of materials based on MMA-MAZ and PMMA matrices*

In two composite materials with different polymer matrices –MMA-MAZ and PMMA – and the same weight content of chromophore-guest AAB-TCV, p^{cc} is somewhat greater in the case of MMA-MAZ/AAB-TCV (20), than in PMMA/AAB-TCV(20) (52% against 42%) (Table 7), $p^{cc}(\pi)$ is almost the same for these two systems. As for the features of H-bonding in these systems (Table 8), the number of HBs between chromophore-guests and polymer chains is very similar (49 against 42) in MMA-MAZ/AAB-TCV(20) and PMMA/AAB-TCV(20), while the p^{cm}(HB) is greater in the case of PMMA/AAB-TCV(20) (84% against 63%).

Earlier [24,32] the energies of HB and π-π stacking between azochromophores were estimated, being of the order of 8 kcal/mole and 13 kcal/mole, respectively; for aromatic HBs it is about 2.8 kcal/mole. When the number of such bonds in the material is significant, they can provide the formation of physical network. The dynamical nature of such reversible bonds [47] (in the course of poling some of them are broken, others arise) makes them promising for fixing the chromophores orientation order. The set of non-covalent bonds in structurally dynamic NLO polymers may be considered as the alternative to polymer cross-linking, which is conventionally used to fix chromophores orientation order achieved by poling. Thus guest-chromophores not only represent the sources of NLO activity but simultaneously serve as cross-linking agents, while the emerging bonds are non-covalent rather than covalent.

3.3.5. ***Glass** transition temperature estimations*

Following the approach developed earlier in [24] for MMA-MAZ, we have performed the estimations of T_g for composite binary chromophore materials based on MMA-MAZ matrix. The results are summarized in Table 9, corresponding graphs with bilinear fits of dependence of specific volume on temperature are given in Fig. 9.

In polymer science it is assumed that introduction of guests in polymer matrix usually results in T_g decrease, since guests serve as loosening agents. However, this tendency is affected by the size and nature of a matrix and chromophore (in particular, acceptor moiety), chromophore content and the presence of noncovalent bonding with polymer matrix. The obtained data demonstrate that in composite systems the T_g value increases due to a large number of non-covalent H-bonds between various components: chromophores and polymer chains. It elucidates the effect of physical network formation on the thermophysical characteristics of polymer composite material.

Table 8
Number of HBs in MMA-MAZ/AAB-TCV(20) and PMMA/AAB-TCV(20), arising during 20 ns at 400 K (the range and average values).

		MMA-MAZ/AAB-TCV(20)	PMMA/AAB-TCV(20)
N		78	50
N_b(HB)_total	range	85–130	34–65
	mean	106	51
N(MMA-MAZ-MMA-MAZ)	range	22–48	–
	mean	35	–
N(AAB-TCV-AAB-TCV)	range	13–32	1–18
	mean	22	9
	p^{cc}(HB), %	56	36
N (AAB-TCV–MMA-MAZ)	range	31–66	29–58
	mean	49	42
	p^{cm}(HB), %	63	84

Table 9
Glass transition temperature, T_g, for several studied systems.

Polymer systems	Tg, K
MMA-MAZ	431
MMA-MAZ/AAB-TCP(10)	448
MMA-MAZ/AAB-TCP(20)	447
MMA-MAZ/AAB-TCP(30)	426
MMA-MAZ/AAB-TCV(30)	449

4. Conclusion

In the present work the atomistic modeling of methacrylate-based composite polymer materials with azochromophores as guests is performed. Polymer matrices are PMMA, copolymer of methyl methacrylate and methacrylic acid, MMA-MAA, and copolymer of MMA and MAZ, MMA-MAZ, MAZ unit containing azochromophore with nitro-group as acceptor, covalently attached to the side chain; guest azochromophores contain various acceptor moieties: NO_2, DCV, TCV and TCP. The content of chromophors-guests in the material is 10, 20 and 30 wt%. The relationship between chromophore structure, concentration, the nature of host matrix and realization of non-covalent interactions of various types is analyzed.

It is shown that up to 30 wt% content of chromophores, their uniform distribution in the material is retained, various non-covalent bonds are formed – hydrogen bonds and π-π-stacking, their number increasing with the growth of the chromophores concentration.

Analysis of non-covalent bonds between chromophores-guests showed that the number of bonds is determined mostly by the nature of the acceptor group, the maximum number is achieved for AAB-TCP chromophores in MMA-MAA matrix.

PMMA and MMA-MAA matrices allow realization of similar number of HBs between matrix and guests at the same content of chromophores, the main difference between these two matrices is the absence of non-covalent bonding between chains in PMMA. Regardless of the acceptors, in PMMA-based materials the proportion of H-bonded chromophores, p^{cc}(HB), increases, while the proportion of chromophores H-bonded with polymer matrix, p^{cm}(HB), decreases with chromophore content. The proportion of π-π-coupled chromophores, $p^{cc}(\pi)$, is shown to be greater than the proportion of H-bonded chromophores, p^{cc}(HB), and its growth with chromophore content is more pronounced than that of p^{cc}(HB); so chromophores are mostly bound inter se by π-π interactions, than by HBs. For composite materials based on MMA-MAA the situation depends on the nature of the acceptor: for AAB-NO_2 guests the similar tendency is observed, while for AAB-TCP guest interchromophore HBs dominate due to greater number of sites for H-bonding in TCP.

In MMA-MAZ/AAB-TCV(20) composite material a great number of non-covalent bonds are realized between host polymer chains, host and guests, and between guests, the comparable proportion of π-π and H-bonds is revealed. AAB-TCV chromophores somewhat more easily interact via π-π bonding with MAZ units than with each other ($p^{cm}(\pi)$ being somewhat greater than $p^{cc}(\pi)$), at that MAZ units more easily interact with AAB-TCV guests than with other MAZ chromophores ($p^{cm}(\pi)$ being somewhat greater than $p^{mm}(\pi)$). As for HBs, the proportion

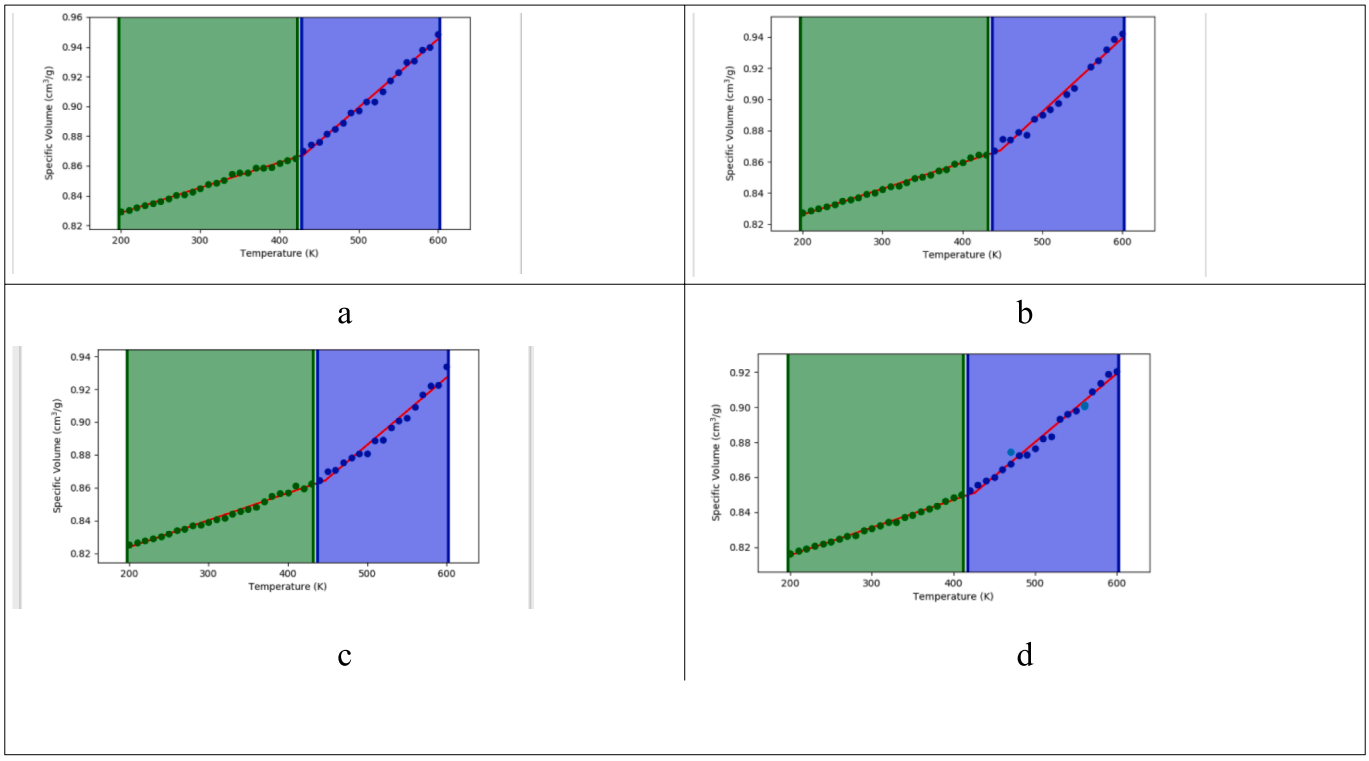

Fig. 9. The dependence of the specific volume on temperature for MMA-MAZ (a), MMA-MAZ/AAB-TCP(10) (b), MMA-MAZ/AAB-TCP(20) (c), MMA-MAZ/AAB-TCP (30) (d).

of AAB-TCV bound with each other is close to that of HBs with polymer chain.

The estimation of the T_g value for composite MMA-MAZ/AAB-TCP demonstrates its increase in comparison with T_g for the MMA-MAZ matrix due to a large number of non-covalent H-bonds in the composite.

Thus, a variety of non-covalent bonds revealed in all the studied composite systems may serve a physical network that could contribute to fixing the chromophores polar order and provide relaxation stability of quadratic NLO response.

CRediT authorship contribution statement

O.D. Fominykh: Formal analysis, Methodology, Writing – original draft. **A.V. Sharipova:** Data curation, Formal analysis, Visualization. **M. Yu. Balakina:** Formal analysis, Investigation, Project administration, Supervision, Writing – review & editing.

Declaration of Competing Interest

The authors declare that they have no known competing financial interests or personal relationships that could have appeared to influence the work reported in this paper.

Acknowledgement

Financial support of Russian Foundation for Basis Research (grant number 19-03-00232a) is gratefully acknowledged.

Data availability

The data required to reproduce these findings cannot be shared due to technical limitations.

Appendix A. Supplementary data

Supplementary data to this article can be found online at https://doi.org/10.1016/j.commatsci.2021.110909.

References

[1] P. Ed, Guenter, Nonlinear Optical Effects and Materials, Springer, Berlin, 2002.
[2] L.R. Dalton, P. Gunter, M. Jazbinsek, O.-P. Kwon, P.A. Sullivan, Organic Electro-Optics and Photonics, Polymers and Crystals, University Press, Cambridge, Molecules, 2015.
[3] L.R. Dalton, P.A. Sullivan, D.H. Bale, Electric field poled organic electro-optic materials: state of the art and future prospects, Chem. Rev. 110 (1) (2010) 25–55, https://doi.org/10.1021/cr9000429.
[4] W. Heni Y. Kutuvantavida C. Haffner H. Zwickel C. Kieninger S. Wolf M. Lauermann Y. Fedoryshyn A.F. Tillack L.E. Johnson D.L. Elder B.H. Robinson W. Freude C. Koos J. Leuthold L.R. Dalton 4 7 2017 1576 1590.
[5] C. Kieninger, Y. Kutuvantavida, D.L. Elder, S. Wolf, H. Zwickel, M. Blaicher, J. N. Kemal, M. Lauermann, S. Randel, W. Freude, L.R. Dalton, C. Koos, Ultra-high electro-optic activity demonstrated in a silicon-organic hybrid modulator, Optica 5 (2018) 739–748, https://doi.org/10.1364/OPTICA.5.000739.
[6] J. Wu, Z. Li, J. Luo, A.-Y. Jen, High-performance organic second- and third-order nonlinear optical materials for ultrafast information processing, J. Mater. Chem. C 8 (43) (2020) 15009–15026, https://doi.org/10.1039/D0TC03224G.
[7] D.M. Burland, R.D. Miller, C.A. Walsh, Second-order nonlinearity in poled-polymer systems, Chem. Rev. 94 (1) (1994) 31–75.
[8] F. Liu, Z. Zhai, W. Shi, L. Feng, Z. Wang, G. Qin, M. Peng, Z. Li. Rational enhancement of electro-optic activity:Design and synthesis of cyanoacetate containing nonlinear optical chromophores Dyes Pigm. 185 (2021) 108914. https://doi.org/10.1016/j.dyepig.2020.108914.
[9] Y. He, L. Chen, H. Zhang, Z. Chen, F. Huo, B. Li, Z. Zhen, X. Liua, S. Bo, A novel bichromophore based on julolidine chromophores with enhanced transferring efficiency from hyperpolarizability b to electro-optic activity, J. Mater. Chem. C 6 (2018) 1031–1037, https://doi.org/10.1039/C7TC04928E.
[10] T.-D. Kim, J.-W. Kang, J. Luo, S.-H. Jang, J.-W. Ka, N. Tucker, J.B. Benedict, L. R. Dalton, T. Gray, R.M. Overney, D.H. Park, W.N. Herman, A.-K.-Y. Jen, Ultralarge and Thermally Stable Electro-Optic Activities from Supramolecular Self-Assembled Molecular Glasses, J. Am. Chem. Soc. 129 (2007) 488–489.
[11] W. Wu, Z. Xu, Y. Xiong, S. Xin, H. Tang, C. Ye, G. Qiu, J. Qina, Z. Li, The self-assembly effect in NLO polymers containing isolation chromophores: enhanced NLO coefficient and stability, New J. Chem. 37 (2013) 1789–1796, https://doi.org/10.1039/c3nj00048f.

[12] H. Xu, F. Liu, D.L. Elder, L.E. Johnson, Y. de Coene, K. Clays, B.H. Robinson, L. R. Dalton, Ultrahigh Electro-Optic Coefficients, High Index of Refraction, and Long-Term Stability from Diels-Alder Cross-Linkable Binary Molecular Glasses, Chem. Mater. 32 (4) (2020) 1408–1421, https://doi.org/10.1021/acs.chemmater.9b0372510.1021/acs.chemmater.9b03725.s001.

[13] A.W. Harper, S. Sun, L.R. Dalton, S.M. Garner, A. Chen, S. Kalluri, W.H. Steier, B. H. Robinson, Translating microscopic optical nonlinearity into macroscopic optical nonlinearity: the role of chromophore–chromophore electrostatic interactions, J. Opt. Soc. Am. B 15 (1998) 329–337, https://doi.org/10.1364/JOSAB.15.000329.

[14] M. Makowska-Janusik, J.-F. Benard, Determination of the macroscopic optical properties for composite materials, J. Phys.: Conf. Ser. 79 (2007) 012030, https://doi.org/10.1088/1742-6596/79/1/012030.

[15] L.R. Dalton, A.W. Harper, B.H. Robinson, The role of London forces in defining noncentrosymmetric order of high dipole moment– high hyperpolarizability chromophores in electrically poled polymeric thin films, Proc. Natl. Acad. Sci. USA 94 (10) (1997) 4842–4847.

[16] M.R. Leahy-Hoppa, P.D. Cunningham, J.A. French, L.M. Hayden, Atomistic Molecular Modeling of the Effect of Chromophore Concentration on the Electro-optic Coefficient in Nonlinear Optical Polymers, J. Phys. Chem. A 110 (17) (2006) 5792–5797, https://doi.org/10.1021/jp0565397.

[17] W.K. Kim, L.M. Hayden, Fully atomistic modeling of an electric field poled guest-host nonlinear optical polymer, J. Chem. Phys. 111 (1999) 5212–5222, https://doi.org/10.1364/OTF.1999.SuD8.

[18] M. Makowska-Janusik, H. Reis, M.G. Papadopoulos, I.G. Economou, N. Zacharopoulos, Molecular dynamics simulations of electric field poled nonlinear optical chromophores incorporated in a polymer matrix, J. Phys. Chem. B 108 (2004) 588–596, https://doi.org/10.1021/jp036197+.

[19] H. Reis, M. Makowska-Janusik, M.G. Papadopoulos, Nonlinear Optical Susceptibilities of Poled Guest−Host Systems: A Computational Approach, J. Phys. Chem. B 108 (2004) 8931–8940, https://doi.org/10.1021/jp0498522.

[20] B.H. Robinson, L.R. Dalton, A.W. Harper, A. Ren, F. Wang, C. Zhang, G. Todorova, M. Lee, R. Aniszfeld, S. Garner, A. Chen, W.H. Steier, S. Houbrecht, A. Persoons, I. Ledoux, J. Zyss, A.K.Y. Jen, The molecular and supramolecular engineering of polymeric electro-optic materials, Chem. Phys. 245 (1-3) (1999) 35–50, https://doi.org/10.1016/S0301-0104(99)00079-8.

[21] B.H. Robinson, L.R. Dalton, Monte-Carlo statistical mechanical simulations of the competition of intermolecular electrostatic and poling-field interactions in defining macroscopic electro-optic activity for organic chromophore/polymer materials, J. Phys. Chem. A. 104 (20) (2000) 4785–4795, https://doi.org/10.1021/jp993873s.

[22] N.A. Nikonorova, M.Y. Balakina, O.D. Fominykh, M.S. Pudovkin, T.A. Vakhonina, R. Diaz-Calleja, A.V. Yakimansky, Dielectric Spectroscopy and Molecular Dynamics of Epoxy oligomers with covalently bonded nonlinear optical chromophores, Chem. Phys. Letters 552 (2012) 114–121, https://doi.org/10.1016/j.cplett.2012.09.053.

[23] D. Jungbauer, I. Teraoka, D.Y. Yoon, B. Reck, J.D. Swalen, R. Twieg, C.G. Willson, Second order nonlinear optical properties and relaxation characteristics of poled linear epoxy polymers with tolane chromophores, J. Appl. Phys. 69 (12) (1991) 8011–8017, https://doi.org/10.1063/1.347497.

[24] O.D. Fominykh, A.V. Sharipova, M.Yu. Balakina, Atomistic modeling of polymer materials based on methacrylic copolymers with azochromophores in the side chain, Comp.Mat.Sci. 168 (2019) 32–39, https://doi.org/10.1016/j.comm.mat.sci.2019.05.057.

[25] S.V. Shulyndin, T.A. Vakhonina, G.A. Estrina, B.A. Rozenberg, M.B. Zuev, Synthesis, Structure, and Properties of Bifunctional Azobenzene Monomers and Polymers on Their Basis, Polymer Science, Ser. A 49 (7) (2007) 782–794, https://doi.org/10.1134/S0965545X07070036.

[26] O.D. Fominykh, A.A. Kalinin, S.M. Sharipova, A.V. Sharipova, T.I. Burganov, M. A. Smirnov, T.A. Vakhonina, A.I. Levitskaya, A.A. Kadyrova, N.V. Ivanova, A. R. Khamatgalimov, I.R. Nizameev, S.A. Katsyuba, M.Y. Balakina, Composite materials containing chromophores with 3,7-(di)vinylquinoxalinone π-electron bridge doped into PMMA: Atomistic modeling and measurements of quadratic nonlinear optical activity, Dyes Pigm. 158 (2018) 131–141, https://doi.org/10.1016/j.dyepig.2018.05.033.

[27] O.D. Fominykh, A.A. Kalinin, A.V. Sharipova, A.I. Levitskaya, M.Y. Balakina, The effect of various substituents in donor moiety on the aggregation of nonlinear-optical quinoxaline-based chromophores in composite polymer materials, Comp. Mat. Sci. 183 (2020) 109900, https://doi.org/10.1016/j.commatsci.2020.109900.

[28] L.R. Dalton, D.L. Elder, L.E. Johnson, A.F. Tillack, B.H. Robinson, 25 Years of Organic Electro-Optics and Future Prospects, NLOQO 50 (2019) 67–90.

[29] A.C. Mitus, M. Saphiannikova, W. Radosz, V. Toshchevikov, G. Pawlik, Modeling of Nonlinear Optical Phenomena in Host-Guest Systems Using Bond Fluctuation Monte-Carlo Model: A Review, Materials 14 (2021) 1454, https://doi.org/10.3390/ma14061454.

[30] A. Sugita, Y. Sato, K. Ito, K. Murakami, Y. Tamaki, N. Mase, Y. Kawata, S. Tasaka, Second-Order Nonlinear Optical Susceptibilities of Nonelectrically Poled DR1−PMMA Guest−Host Polymers, J. Phys. Chem. B 117 (47) (2013) 14857–14864, https://doi.org/10.1021/jp407892b.

[31] S. Di Bella, M.A. Ratner, T.J. Marks, Design of Chromophoric Molecular Assemblies with Large Second-Order Optical Nonlinearities. A Theoretical Analysis of the Role of Intermolecular Interactions, J. Am. Chem. Soc. 114 (1992) 5842–5849.

[32] K.Y. Suponitsky, A.E. Masunov, Supramolecular step in design of nonlinear optical materials: effect of π···π stacking aggregation on hyperpolarizability, J. Chem. Phys. 139 (9) (2013) 094310, https://doi.org/10.1063/1.4819265.

[33] O.D. Fominykh, A.V. Sharipova, M.Yu. Balakina, The choice of appropriate density functional for the calculation of static first hyperpolarizability of azochromophores and stacking dimers, Int. J. Quant. Chem. 116 (2) (2016) 103–112, https://doi.org/10.1002/qua.25029.

[34] N.I. Shalin O.D. Fominykh M.Y. Balakina 120 1 2020 10.1002/qua.v120.1 10.1002/qua.26061.

[35] J.M. Cole, Enumerating Intramolecular Charge Transfer in Conjugated Organic Compounds, J. Chem. Inf. Model. 60 (12) (2020) 6095–6108, https://doi.org/10.1021/acs.jcim.0c00913.

[36] J. Vapaavuori, J.E. Koskela, X. Wang, R.H.A. Ras, A. Priimagi, C.G. Bazuin, C. Pellerin, Effect of hydrogen-bond strength on photoresponsive properties of polymer-azobenzene complexes, Can. J. Chem. 98 (9) (2020) 531–538.

[37] J. Contreras-García, E.R. Johnson, S. Keinan, R. Chaudret, J.-P. Piquemal, D. N. Beratan, W. Yang, NCIPLOT: A program for plotting noncovalent interaction regions, J. Chem. Theory. Comput. 7 (3) (2011) 625–632, https://doi.org/10.1021/ct100641a.

[38] E.R. Johnson, S. Keinan, P. Mori-Sánchez, J. Contreras-García, A.J. Cohen, W. Yang, Revealing noncovalent interactions, J. Amer. Chem. Soc. 132 (18) (2010) 6498–6506, https://doi.org/10.1021/ja100936w.

[39] L.R. Dalton, Organic electro-optic materials, Pure. Appl. Chem. 76 (2004) 1421–1433, https://doi.org/10.1351/pac200476071421.

[40] M. Leolukman, P. Paoprasert, I. Mandel, S.J. Diaz, D.J. Mcgee, P. Gopalan, Linear-dendritic block copolymer hosts for the encapsulation of electro-optic chromophores via H-Bonding, J. Polym. Sci., Part A: Polym. Chem. 47 (19) (2009) 5017–5026, https://doi.org/10.1002/pola.v47:1910.1002/pola.23554.

[41] K.H. DuBay, M.L. Hall, T.F. Hughes, C. Wu, D.R. Reichman, R.A. Friesner, Accurate force field development for modeling conjugated polymers, J. Chem. Theory Comput. 8 (11) (2012) 4556–4569, https://doi.org/10.1021/ct300175w.

[42] E. Harder, W. Damm, J. Maple, C. Wu, M. Reboul, J.Y. Xiang, L. Wang, D. Lupyan, M.K. Dahlgren, J.L. Knight, J.W. Kaus, D.S. Cerutti, G. Krilov, W.L. Jorgensen, R. Abel, R.A. Friesner, OPLS3: a force field providing broad coverage of drug-like small molecules and proteins, J. Chem. Theory Comput. 12 (1) (2016) 281–296, https://doi.org/10.1021/acs.jctc.5b0086410.1021/acs.jctc.5b00864.s001.

[43] A. Khachaturyan, S. Semenovsovskaya, B. Vainshtein, The thermodynamic approach to the structure analysis of crystals, Acta Crystallogr. A 37 (5) (1981) 742–754, https://doi.org/10.1107/S0567739481001630.

[44] Leslie H. Sperling (Ed.), Introduction to Physical Polymer Science, fourth ed., Wiley-Interscience, A John Wiley&Sons, Inc., Hoboken, New Jersey, 2006, p. 668.

[45] L.L.C. Schrödinger, . NY (Eds.), Materials Science Suite 2021–1, 2021.

[46] Schrödinger Release 2021–1, Desmond Molecular Dynamics System, D. E. Shaw Re-search, New York, NY, 2020 Maestro-Desmond Interoperability Tools, Schrödinger, New York, NY, 2021.

[47] Jean-Marie Lehn, Perspectives in Chemistry—Steps towards Complex Matter, Angew. Chem. Int. Ed. 52 (10) (2013) 2836–2850, https://doi.org/10.1002/anie.201208397.